OPEN ACCESS

University of BRISTOL

Magi, F., Di Maio, D., & Sever, I. (2016). Damage initiation and structural degradation through resonance vibration: Application to composite laminates in fatigue. *Composites Science and Technology*, *132*, 46-57. https://doi.org/10.1016/j.compscitech.2016.06.013

Peer reviewed version

License (if available):
CC BY-NC-ND

Link to published version (if available):
10.1016/j.compscitech.2016.06.013

Link to publication record in Explore Bristol Research
PDF-document

This is the author accepted manuscript (AAM). The final published version (version of record) is available online via Elsevier at doi:10.1016/j.compscitech.2016.06.013. Please refer to any applicable terms of use of the publisher.

University of Bristol - Explore Bristol Research
General rights

This document is made available in accordance with publisher policies. Please cite only the published version using the reference above. Full terms of use are available:
http://www.bristol.ac.uk/red/research-policy/pure/user-guides/ebr-terms/

Damage initiation and structural degradation through resonance vibration: application to composite laminates in fatigue

Fabrizio Magi[a], Dario Di Maio[b,*], Ibrahim Sever[c]

[a] *Advanced Composites Centre for Innovation & Science, University of Bristol, UK*
[b] *Department of Mechanical Engineering, University of Bristol, Bristol, UK*
[c] *Rolls-Royce plc, Derby, DE24 8BJ, UK*

Abstract

The definition of failure is fundamental to the characterisation of fatigue strength of components and structures and is often expressed as a percentage of stiffness degradation. This article proposes a new method to capture damage initiation and structural degradation during a fatigue test, by exploiting resonance vibrations. The method entails monitoring dynamic parameters, including the phase angle between excitation and response, which suddenly changes as soon as the overall stiffness changes as a consequence of damage. In this paper, a theoretical approach based on equations of motion is presented in order to describe the possible scenarios in which a component undergoes structural degradation. In the proposed approach, an abrupt change in the time history of the stiffness of the component is assumed and analysed in both the quasi-static case at low excitation frequencies and the dynamic case, when the excitation frequency is close to the resonance frequency. The resulting analytical solution shows that any small stiffness variation is amplified by the dynamic response of the component as a large phase change, even when it is too small to be captured by the quasi-static response. The idea is successfully applied to capture the initiation of delamination in CFRP laminates, and the relative S-N curve to initiation is drawn. The experimental evidence of a critical event in the fatigue life of a component is found both in the dynamic phase response and in the base acceleration. The critical event is captured from a sudden change in the dynamic parameters of the structure as soon as a delamination is initiated. Thermography, C-scan and micrograph confirmed that the onset of delamination occurs at the moment of the critical event, after an initial stage of microcracking.

Keywords: Initiation, Fatigue, Resonance testing, Structural degradation, Failure criterion

1. Introduction

The definition of damage initiation is one of the most discussed topics in fatigue behaviour of components. It is widely agreed that the nucleation of damage in a pristine component can be a large part of its total fatigue life, but unfortunately its characteristic features are particularly

*Corresponding author
Email address: Dario.DiMaio@bristol.ac.uk (Dario Di Maio)

difficult to understand and therefore predict. For this reason, the crack initiation is usually related to a subjective critical crack dimension. For different materials, as recalled by Bhattacharya et al. [1] , the critical crack dimension could vary from a microscopic scale of few micrometres [2] to a few millimetres, depending on the type of components or structures and their applications. The lack of a generally accepted definition of crack initiation can be put down to (i) the difficulty of measuring cracks on the length scale of nanometres and (ii) the practical significance of having measured a crack of such small size.

As the definition of crack initiation is not unique for homogeneous materials, such as metals, it is even harder to find a general definition of initiation for composite materials, where damage is identified by the complex status of the material rather than by a single crack. Since first studies on fatigue of composites, it was clear that the damage development comprised a series of interacting phenomena, leading to continuous and diffuse structural degradation. Reifsnider in 1980 addressed the main issue in understanding fatigue behaviour of composites, i.e. the absence of a "well-defined damage state, something that replaces a single crack in homogeneous materials" [3]. He proposed a sequence of steps for the damage development that can be summarised as (i) crack nucleation in off-axis plies and saturation at the Characteristic Damage State, (ii) crack coupling due to the interface debonding when the crack tips reach the interfaces, (iii) formation of a wider damaged region by the previous process, (iv) crack growing through the thickness by crack coupling and (v) final fracture of fibres in the direction of the load.

According to this sequence, the damage initiation should be defined as the first nucleation of a transverse crack in an off-axis ply. However, initiation could be defined at different levels, from the microscopic molecular observation level to the macroscopic structural observation level. As demonstrated by Caiulo and Kachanov [4], there is no direct correlation between clustering of microcracks (microscopic observation level) and stiffness reduction (structural level). In fact, since the stiffness reduction is a property of the entire structure, it averages the crack distribution over the volume, resulting in being insensitive to clustering. Therefore, a more practical definition of initiation is the one given by Salkind [5] as "the time required to form a crack of detectable size". Lomov et al. [6] considered the damage initiation as the occurrence of a crack that connects many debonded fibres and that can be captured by an increase in the energy content of acoustic emissions. Quaresimin [7] used 0.3 mm as the value of the crack to be considered detectable by a microscope, justifying that small changes in the initial crack length have a small effect on the fatigue life, within the scatter of the experimental data in any case. On the other hand, O'Brian proposed a new damage tolerance philosophy for composite materials [8], assuming the existence of matrix cracks throughout the off-axis plies, and the onset of delamination being predicted by a strain energy release rate threshold. This threshold can be obtained by running several tests at several high loads, whereby the onset of delamination is always unstable and easily detectable because of catastrophic change in stiffness. In Ref. [9], Sims reviewed the fatigue testing methods

beginning with the concept of failure criterion for composites. He identified the need for a failure criterion based on loss of stiffness, as recommended by standard procedures [10], that could vary from 5% to 20%, depending on applications. It is evident, once again, that there is no universal criterion to define the damage initiation.

May and Hallett [11] investigated the incorporation of damage initiation into a cohesive element model. In this case, model calibrations were made for mode I and mode II in accordance with the previous work of O'Brien et al. [12] on transverse tension fatigue and May and Hallett [13] on damage initiation in shear fatigue, respectively. For mode I it was observed that initiation and final failure occurred within a short period of time, thus it was assumed that initiation corresponded to the actual separation of the specimen in two pieces. For mode II, the Short Beam Shear (SBS) test and the Double Notched Shear (DNS) test were evaluated and compared for their potential in providing data for S-N curves to damage initiation. Both tests have some shortcomings and limitations, but it was concluded that the DNS test was more reliable in determining damage initiation.

Use of resonance vibration for in-situ monitoring of structural degradation and residual stiffness of components during fatigue testing is not new [14–16]. Since first studies in the 50's [17], the vibration fatigue testing method has become standard practice [18, 19], exploiting the resonance conditions to perform quick tests to a high degree of accuracy, even in the Very High Cycle Fatigue (VHCF) regime, up to the gigacycle [20].

In the present work it is shown how a measurement of the resonance frequency or a direct measurement of the stiffness could be too coarse to capture the occurrence of damage initiation during the test. The aim of this article is to present a more sensitive method for monitoring structural degradation and consequently damage initiation. Here, damage initiation shall be defined as a critical event that changes the rate of structural degradation for a given excitation level. In other words, an event that can abruptly change the distribution of the stiffness of a component under fatigue loading conditions.

2. Understanding structural degradation in a dynamic environment

Let us consider a prismatic beam of length L and section S subjected to longitudinal natural vibration. The forces acting on an infinitesimal segment of the beam in Fig. 1 having density ρ and length dx can be written as

$$\frac{\partial F}{\partial x}dx = \rho S dx \frac{\partial^2 u}{\partial t^2}, \tag{1}$$

where F is the force, u is the displacement and t is the time. By considering the definition of the elastic modulus, one can write

$$\frac{F}{S} = \sigma = E\varepsilon = E\frac{\partial u}{\partial x}. \tag{2}$$

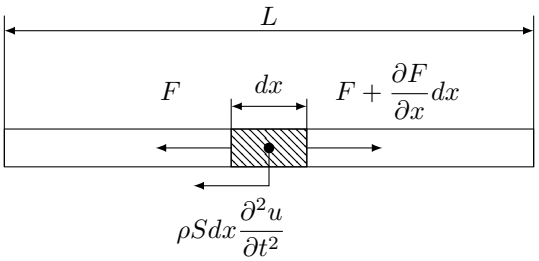

Figure 1: Forces acting on an infinitesimal beam segment subjected to longitudinal natural vibration.

Combining Eq. (1) with Eq. (2) yields to

$$\frac{\partial^2 u}{\partial x^2} = \frac{\rho}{E} \frac{\partial^2 u}{\partial t^2}, \tag{3}$$

where the ratio between the density ρ and the Young's modulus E is the inverse of the velocity of propagation of the strain wave in the beam, ν.

For a free-free beam the solution of the n^{th} mode of vibration gives an angular frequency ω that can be written in the form

$$\omega = \frac{n\pi}{L} \sqrt{\frac{E}{\rho}}, \tag{4}$$

Eq. (4) for the first mode ($n = 1$) reduces to

$$\omega = \frac{\pi}{L} \sqrt{\frac{ESL}{\rho SL}} = \pi \sqrt{\frac{k}{m}}, \tag{5}$$

where $m = \rho SL$ is the mass of the beam and $k = ES/L$ is the axial stiffness. One can relate this example to a simpler Single Degree Of Freedom (SDOF) system. For our scope of showing the high sensitivity of the phase in capturing any change in the stiffness of the structure, it is necessary to add a damping force to the system. A typical lumped parameters SDOF system is given by a mass-spring-damper arrangement, where a mass is connected to the ground by a spring and a damper in parallel. The mass is excited by a force acting directly on it, and the response is measured as the absolute displacement of the mass. This SDOF system is well known. We shall focus on the solution of the forced response. The modulus of the receptance $\alpha(\omega)$ and the phase shift $\varphi(\omega)$ can be described by the relationships

$$|\alpha(\omega)| = \frac{|X|}{|F|} = \frac{1}{\sqrt{(k - \omega^2 m)^2 + (\omega c)^2}}, \tag{6a}$$

$$\varphi(\omega) = \tan^{-1} \frac{\omega c}{k - \omega^2 m}, \tag{6b}$$

where X is the response in terms of displacement, F the excitation force, k the spring stiffness, m the mass and c the damping coefficient. From the sensitivity analysis of the phase expressed in Eq. (6b), and with reference to Fig. 2, it is possible to see why resonance frequency is not a suitable parameter to measure the structural degradation. The resonant frequency reduction for a

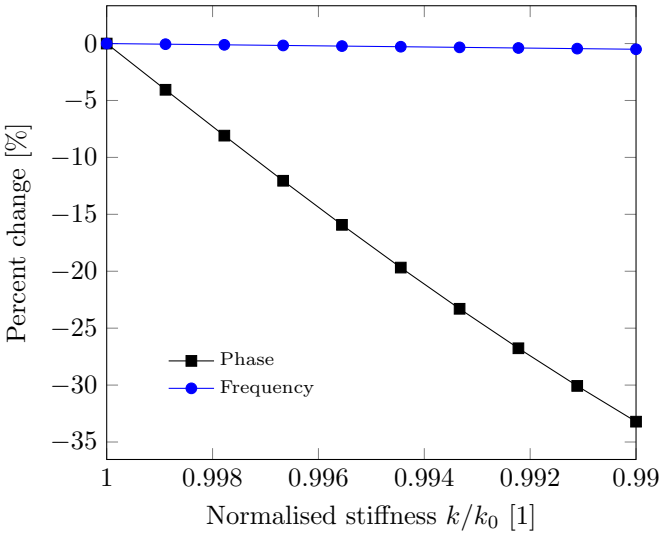

Figure 2: Comparison between change in resonant frequency and change in phase for a small change in stiffness of a SDOF system with 1% damping.

decrease in stiffness of 1% is 0.5% at constant phase, while a phase shift at constant frequency is about 34%. These values are obtained for a system with 1% of damping. Thus, considering that the resonant frequency is proportional to the square root of the stiffness, it is even less sensitive to structural degradation than the stiffness itself. Fig. 3 shows the change in response phase of an SDOF system having an initial stiffness k_0 of 4.5 Nm^{-1} and a mass of 6.8×10^{-6} kg. The system is subjected to a constant excitation frequency $\omega = \sqrt{k_0/m}$ whilst the stiffness is gradually reduced by 1%[1] for many different damping ratios. In this case it is shown that a decrease in stiffness of 1% results in a greater than 30% decrease in phase for a damping ratio lower than 2%. Obviously, the higher the damping the less sensitive the phase becomes. Even then, for a damping ratio as high as 8% there is still an effect on the phase three times greater than the relative decrease in stiffness.

It is trivial to see that by fatiguing the component, any change in the structure will cause a change in stiffness, which in turn will modify the dynamics of the system. By the same principle, also the static response of the system will be modified. However, in contrast to the dynamic case, in a quasi-static case the Young's modulus of a linear elastic material relates stresses and strains with no lag.

In order to see how the system response changes for different excitation regimes, we consider a hypothetical bilinear structural degradation law over a normalised time, as shown in Fig. 4. Such behaviour was already assumed by Talreja for modelling the stiffness reduction due to transverse cracks for composites with high degree of constraint [22]. In the considered structural degradation law, the initial stiffness reduction follows a linear law with a gradient of −0.3%. At this rate the

[1] Values for k_0 and m are estimated with Rayleigh's energy method applied to the typical test reported in Ref. [21]. They are the lumped stiffness and mass, respectively, to produce the equivalent SDOF system.

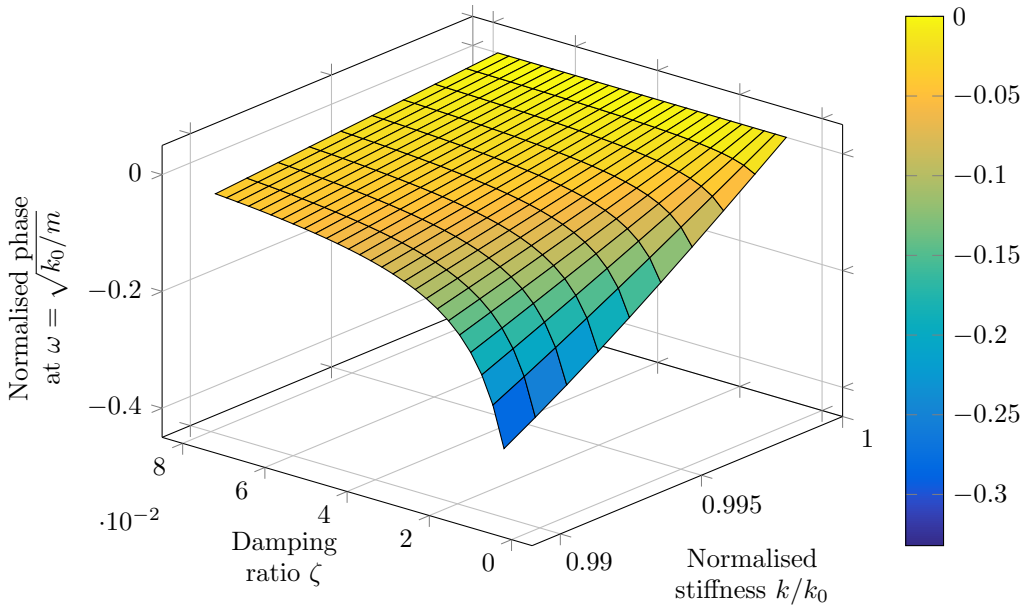

Figure 3: Sensitivity of the phase to changes in stiffness for various damping ratios.

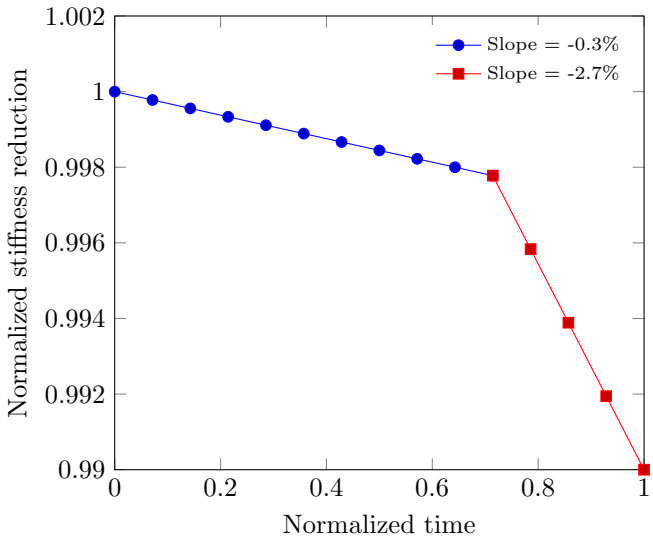

Figure 4: Hypothetical bilinear law for the stiffness reduction over time.

total reduction at the end of the time period would have been -0.3%. However, at 70% of the total time, a major event would have suddenly changed the distribution of stiffness along the component (as a transverse crack would have done in the beam of Fig. 1), and for the last 30% of the total time, the stiffness reduction gradient would increase to -2.7%. By applying the bilinear law to the stiffness k of the SDOF, and plotting the change in the force-displacement relationship over time, one obtains the surface shown in Fig. 5 and 6.

When the system undergoes cyclic excitation, the surface is an elliptical tube slightly rotated about the centre, the eccentricity of which varies as the phase shift and receptance (Fig. 5). The section of the tube on the force-displacement plane is a Lissajous curve defined by the harmonic system of the response $X(t)$ and the excitation $F(t)$

$$\begin{cases} X(t) = x(t) = |X| \sin(\omega t), \\ F(t) = y(t) = \dfrac{|X|}{|\alpha(\omega)|} \sin(\omega t + \varphi). \end{cases} \tag{7}$$

By a change of variables, one can write the system in Eq. (7) as the single function

$$X(F) = x(y) = |X| \sin\left(\arcsin\left(\frac{y}{\dfrac{|X|}{|\alpha(\omega)|}} \right) + \varphi \right). \tag{8}$$

Eq. (8) reduces to canonical forms for $\varphi = 0$ and $\varphi = \pi/2$. When the phase is $\pi/2$ the system is excited in resonance and Eq. (8) can be written as an ellipse with eccentricity e dependent only on receptance:

$$e = \sqrt{1 - \frac{1}{|\alpha|^2}}. \tag{9}$$

By continuously changing the phase towards smaller angles, the ellipse rotates and the eccentricity increases. The ellipse distortion is significant for small deviations of φ from $\pi/2$. This process would drops off for the phase approaching zero (i.e. when the system is excited at frequencies much smaller than the resonant frequency). This case, shown in Fig. 6, represents the quasi-static case, for which Eq. (8) reduces to Hook's linear law when $\omega = 0$

$$x \approx \alpha_{(\omega \ll \omega_n)} y, \tag{10}$$

$$X = \alpha_{(\omega=0)} F = \frac{1}{k} F. \tag{11}$$

3. Damage initiation in CFRP coupons under vibration fatigue loading

Eq. (8) along with Fig. 5 and Fig. 6 show how a small structural degradation affects the behaviour of a component in different excitation environments.

In real fatigue experiments the SDOF model still holds. For a fatigue test carried out in a hydraulic tensile machine at $R = -1$, the case is perfectly represented by the SDOF with the excitation force applied to the mass. However, the exploitation of resonance vibration in that case

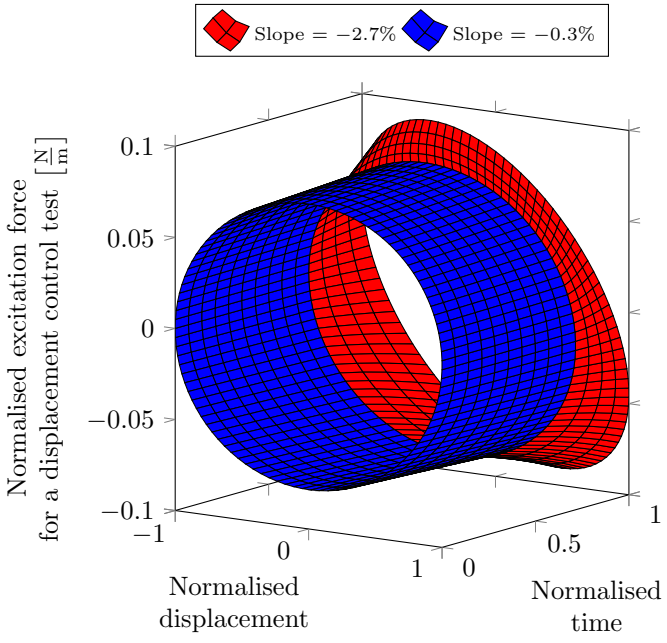

(a)

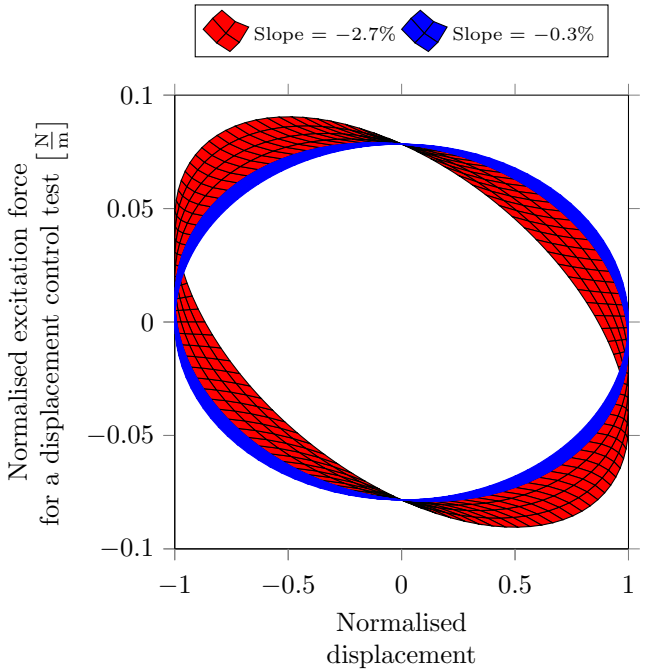

(b)

Figure 5: Changes in system response for a SDOF excited at resonance. Fig. 5a shows the surface envelope over time and Fig. 5b shows the contour. Colours refer to the gradient of the bilinear law in Fig. 4.

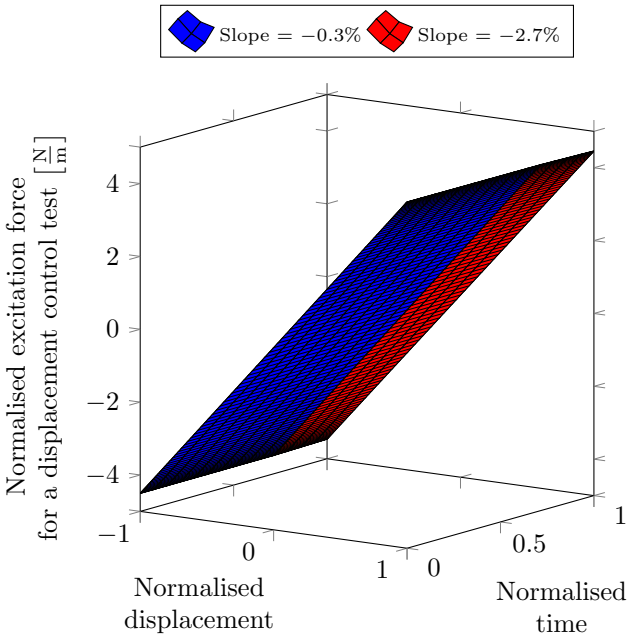

(a)

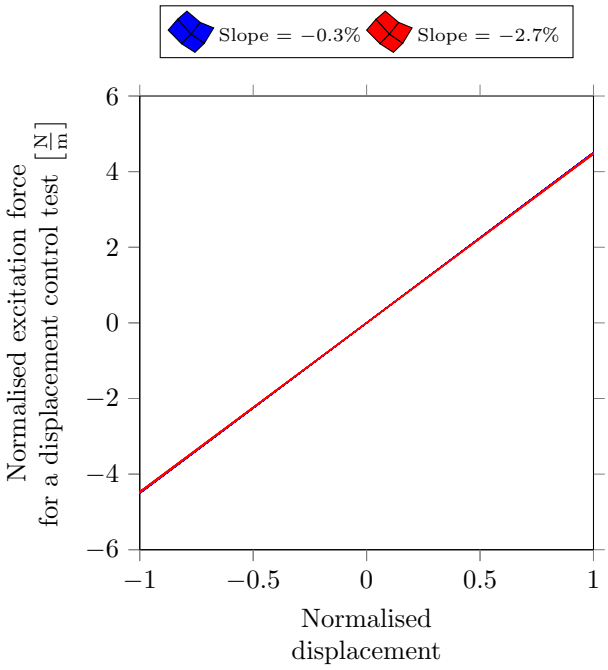

(b)

Figure 6: Changes in system response for a SDOF excited out of resonance. Fig. 6a shows the surface envelope over time and Fig. 6b shows the contour. Colours refer to the gradient of the bilinear law in Fig. 4.

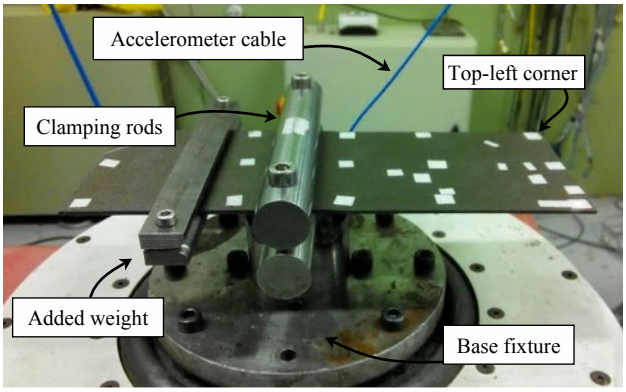

Figure 7: Rig setup.

is rare due to experimental challenges, mainly on account of the excitation frequency limit of the tensile machine and the maximum available force at that frequency.

Nevertheless, a similar configuration could be achieved by means of an electromagnetic shaker exciting a specimen using base excitation. The lumped parameter model of this system is described by a mass connected to a vibrating base through a spring and a damper. The dynamic excitation is given by the displacement of the base as a function of time $X_b(t)$, rather than by a force acting directly on the mass.

The overall idea is still valid but the phase lag and the transmissibility in a base excitation between the base and mass displacement are given by [23]:

$$\varphi(\omega) = \tan^{-1} \frac{mc\omega^3}{k\left(k - \omega^2 m\right) + (\omega c)^2}, \tag{12a}$$

$$|T(\omega)| = \frac{|X|}{|X_b|} = \frac{\sqrt{k^2 + (\omega c)^2}}{\sqrt{\left(k - \omega^2 m\right)^2 + (\omega c)^2}}. \tag{12b}$$

The setup was presented in Ref. [21] and it is summarised, for ease of reading, as follows. Fig. 7 shows a steel fixture clamping the component and connected to the shaker head. In order to minimize friction and to avoid nonlinear boundary conditions, the fixture constrains the component along a line by means of two cylindrical rods. The component is a rectangular specimen 100 mm $\times$ 260 mm, made with 20 pre-preg plies of IM7/8552, 4 of which are interrupted plies 100 mm $\times$ 130 mm. The stacking sequence is $[0, 0_{cut}, 90_{cut}, (0, 90)_3, 0]_s$ and the ply-drop is 20 mm away from the clamp, in the middle of the specimen. The ply-drops are common features for most of the composite components, and they are here introduced to move the maximum stressed area away from the clamp. The stack of plies is vacuum bagged and cured in autoclave according to Hexcel procedures [24]. Strains are measured on the ply-drop by using strain gauges and tests are carried out at resonance (first bending mode), at constant frequency and vibration amplitude by controlling the driving power of the shaker. Specifically, the resonance frequency of the system is

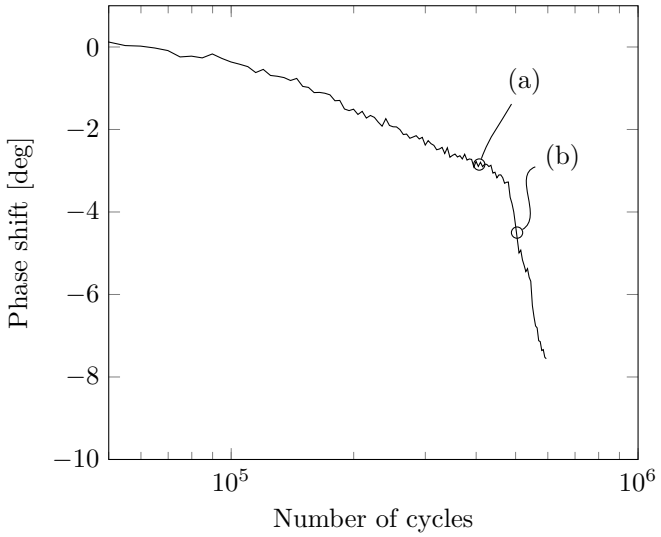

Figure 8: Typical bilinear law in a logarithmic scale for the phase measurement during fatigue. Letters refer to the captions in Fig. 9.

131 Hz ± 1.5%[2], and the loading ratio is $R = -1$. The base acceleration, the velocity of vibration at the tip of the specimen (top-left corner in Fig. 7) and the phase delay between them are measured to feed the control and to capture the initiation of delamination. The phase φ reported in Eq. (12a) will be $\pi/2$ smaller than the measured phase in this set-up configuration. In fact, the signal measured for computing the response phase are the tip velocity V_{mass} and the base acceleration A_{base} instead of the tip displacement X_{mass} and the base displacement X_{base}. In an oscillating system, velocity and displacement are in phase quadrature, whilst acceleration and displacement are in anti-phase.

By focusing on a single fatigue test and by plotting the phase versus the logarithm of the number of cycles, one obtains the graph in Fig. 8, that can be considered as a bilinear law to a first approximation. In addition, exciting the component around the resonance frequency, the first order Taylor expansion of Eq. (12a) can be written as [3]

$$\varphi_{(k=\omega^2 m)} = \tan^{-1}\frac{m\omega}{c} + \frac{m^2\omega\left(k - m\omega^2\right)}{c^3 + cm^2\omega^2} + \mathcal{O}\left(\left(k - m\omega^2\right)^2\right). \tag{13}$$

Eq. (13) shows that the phase is directly proportional to the stiffness for sufficiently small stiffness variations at constant excitation frequency. Therefore, the phase reduction law shown in Fig. 8 can be related to a qualitatively similar bilinear stiffness reduction law, as hypothesised in Fig. 4. One can then infer that a major event has abruptly changed the stiffness of the system.

The critical event – i.e. the major event that changed the distributed stiffness of the system – is attributed to the initiation of the delamination, and it is measured by an abrupt change in

[2]Maximum scatter of the data.

[3]Note that the symbol $\mathcal{O}$ describes the asymptotic behaviour of the Taylor expansion of φ, truncated at terms of order $\left(k - m\omega^2\right)^2$

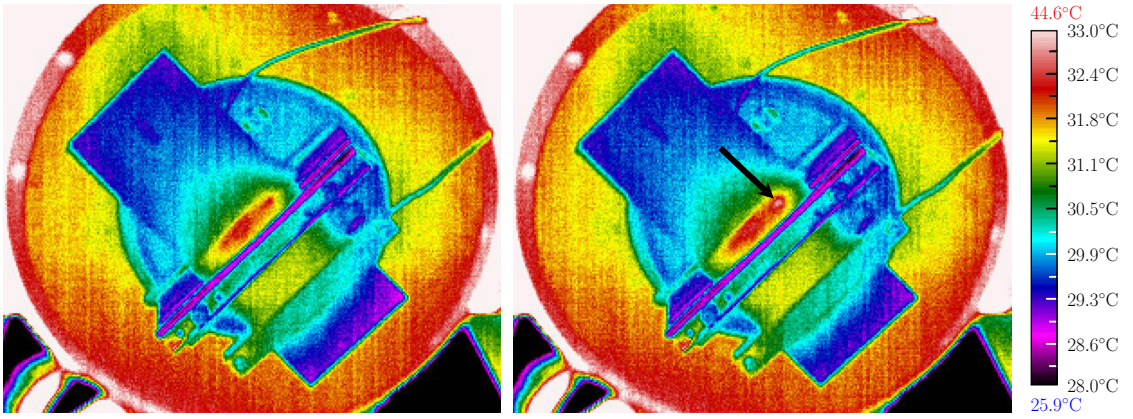

(a) (b)

Figure 9: Thermal images of the top surface of the specimen (a) before and (b) after the critical event. The delamination is indicated by the arrow.

the rate of response phase reduction. In Ref. [21], it is shown that thermal images help with the spatiotemporal characterisation of the onset of delamination in the case of simple specimen testing, therefore they can be used as a proof of the occurrence of a critical event. In fact, referring to Fig. 9, where it is shown the top surface of the specimen, the initiation of delamination is promptly captured because of the local increase in temperature due to the heat dissipated by the friction between delaminated plies. For the discussed case the delamination always initiates between the first and the second ply in the ply-drop location. Therefore, the time lag for the heat to reach the outer surface so that it can be captured by the thermal camera is minimal.

The C-scan of the specimen in Fig. 10 shows where the small delamination occurred. The image is taken from the top of the specimen, over an area 100 mm wide and 80 mm long, crossing the ply-drop for the entire width at 57 mm. The specimen was clamped 20 mm away from the ply-drop, around a horizontal line that would cross the vertical axes of the same image at 37 mm. The delamination occurred around 75 mm from the left edge and has a diameter of approximately 6 mm. Referring to the C-scan in Fig. 10, the specimen was cut along four main lines intersecting the horizontal axes at 70 mm (a), just outside the delaminated area, at 75 mm (b), in the centre of the delamination and at 65 mm (c) and 35 mm (d) both away from the delamination. The micrographs in Fig. 11a, Fig. 11c and Fig. 11d show that away from the delaminated area one can find a single microcrack within the resin pocket, grown through the width of the specimen, as described by Talreja [25]. For every cross section, it is possible to spot that the crack in the resin pocket grows towards the outer ply (Fig. 11c). After reaching the outer ply interface, the crack grows along the interface (Fig. 11d) eventually coupling with neighbour cracks to suddenly form an actual delamination.

These steps, representing the structural degradation of the component, are well described by the two different gradients of the curve in Fig. 8. Up to the critical event the matrix cracking spreads along the resin pocket leading to a very small stiffness reduction, measurable as a change in the

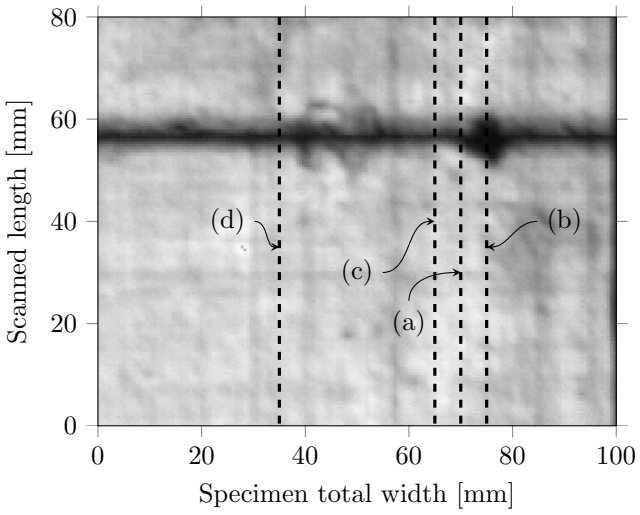

Figure 10: C scan of the specimen with scan resolution 0.5 mm. Dashed lines refer to the cutting plane of the micrographs in Fig. 11.

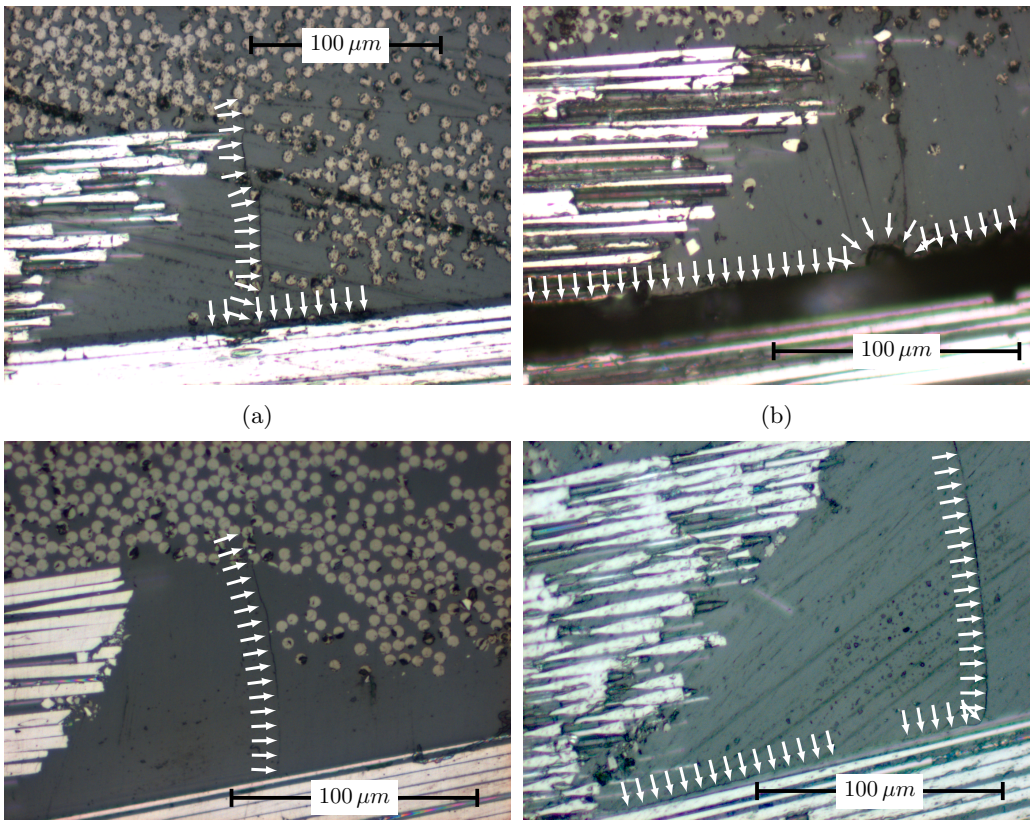

Figure 11: Micrographs of the ply-drops at the cutting plane locations of Fig. 10. Microcracking and delamination marked with arrows.

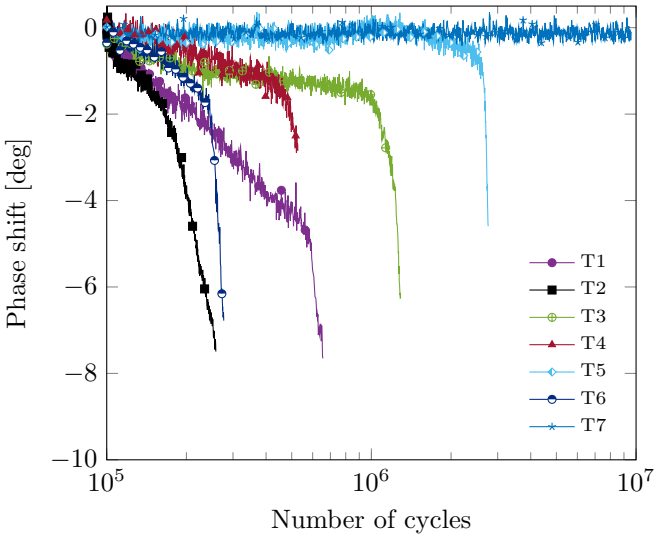

(a)

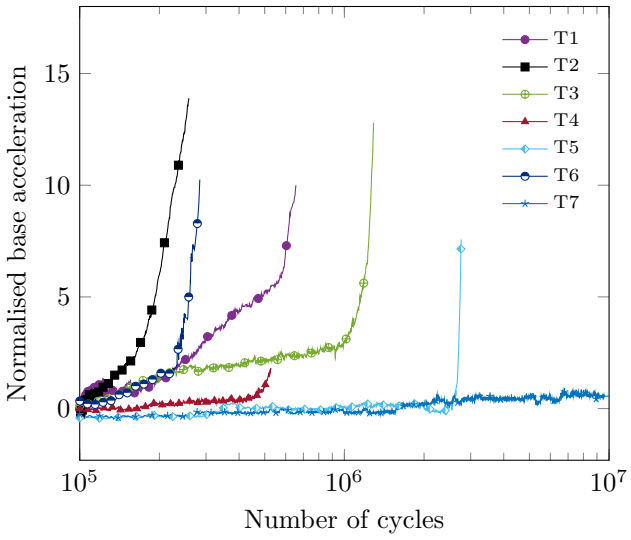

(b)

Figure 12: Bilinear laws in a logarithmic scale for the (a) phase and (b) acceleration during fatigue.

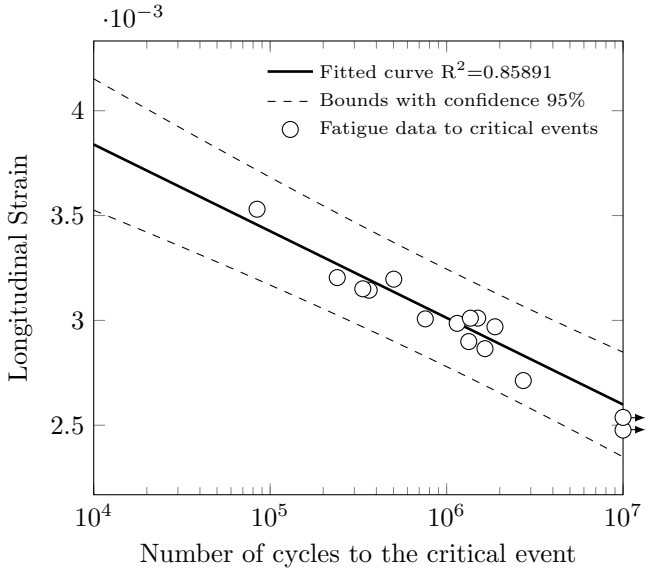

Figure 13: S-N curve by means of strain for the tested component.

phase response of the resonant mode. As soon as the critical event occurs, the phase undergoes a gradient step change, and the stiffness degradation runs faster for the same vibration amplitude. Data are reported for a number of tests in Fig. 12a.

Additionally, from the transmissibility function one can expect the base displacement to exhibit similar behaviour to that of the phase for a constant vibration amplitude, since the Taylor expansion of Eq. (12b) for small variations of k around the resonance frequency is:

$$|T|_{(k=\omega^2 m)} = \sqrt{\frac{m^2\omega^2}{c^2}+1} + \frac{m\left(k-m\omega^2\right)}{c^2+\sqrt{\frac{m^2\omega^2}{c^2}+1}} + \mathcal{O}\left(\left(k-m\omega^2\right)^2\right). \tag{14}$$

Again, the sensitivity of the base displacement is higher than the one of the stiffness, and it is further amplified by considering the base acceleration amplitude, that for a sinusoidal waveform is ω^2 times greater than the displacement. The effect of the critical event on the base acceleration curves is shown in Fig. 12b.

Finally, as a natural consequence of having captured the initiation of the delamination with such precision, the S-N curve by means of strain is drawn (Fig. 13). This S-N curve provides the number of cycles to the first onset of delamination, which can be incorporated in numerical models that predict fatigue life using the Finite Element (FE) method [26], allowing for a more robust design process no longer associated with an engineering consideration.

4. Damage initiation in CFRP component under vibration fatigue loading

To validate the initiation criterion and the method, one fatigue test was performed on a composite blade. The blade was held at the root with a steel fixture, which was bolted down on a shaking table. Due to commercial sensitivities it is not possible for the authors to describe the

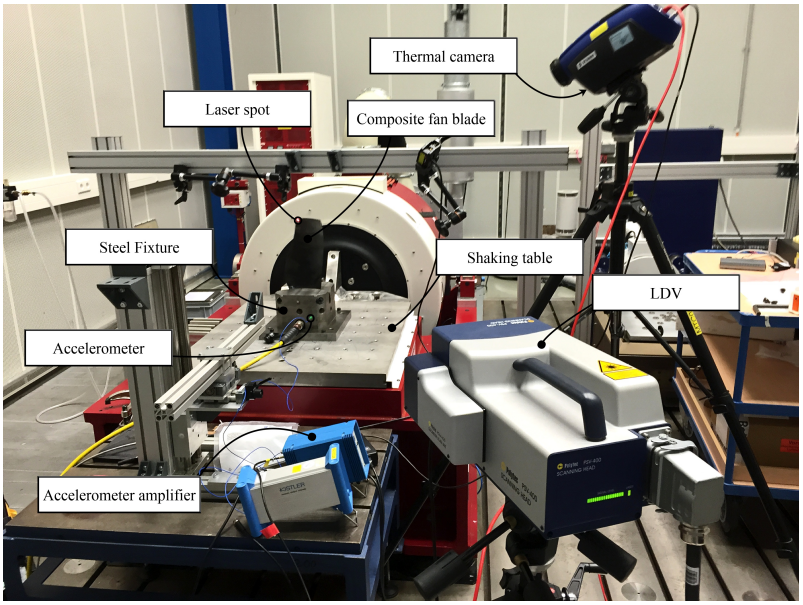

Figure 14: Setup for the vibration fatigue test of the blade.

material composition and the stacking sequence of the blade. The set-up is shown in Fig. 14. The measurement parameters were the same as those for the coupons tests: base acceleration, vibration amplitude at the tip of the blade and temperature. The test was run by exciting the blade at its first bending mode until the critical event occurred.

Referring to Fig. 16, one can observe the same law of the phase for the blade as in coupon tests. The temperature hotspot occurred on the surface at the point of maximum stress, as shown in Fig. 15. However, differently from coupons, the bilinear law of the phase shows its step change in slope a few thousand cycles before the temperature rise. The phase drops before the temperature rise because it is a direct consequence of the structural degradation. As soon as a critical event occurs at one point, it generates a perturbation that spreads over the structure at the sound propagation speed in the material. On the other hand, the heat transfer is slower, resulting in a longer time for the heat to reach the surface of the component. Consequently, looking at the time sequence of the two phenomena in Fig. 16, one can expect the damage to be within the inner plies of the blade. For definitive proof, X-ray Computer Tomography (CT scan) was carried out on the section of the blade where the thermal images showed the hotspot, hence where the damage was expected; the delamination was found to be in the mid-plane of the blade, with a maximum dimension of 6 mm x 4 mm x 1.5 mm.

5. Conclusion

An insight into structural degradation and damage occurrence is given for components that are subjected to vibration fatigue. Fatigue tests carried out in a dynamic environment by exploiting resonance vibrations have the benefit of being very sensitive to the damage, even if it is present in small amounts. Phase and base acceleration are proven to be more sensitive in capturing

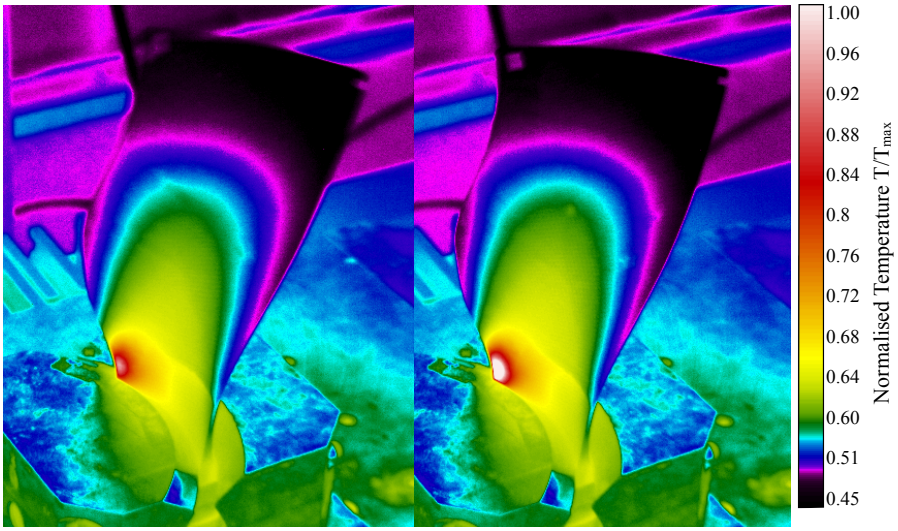

Figure 15: Thermal images for the blade (left) before and (right) after the critical event occurred. The temperature hotspot occurred in the damaged zone.

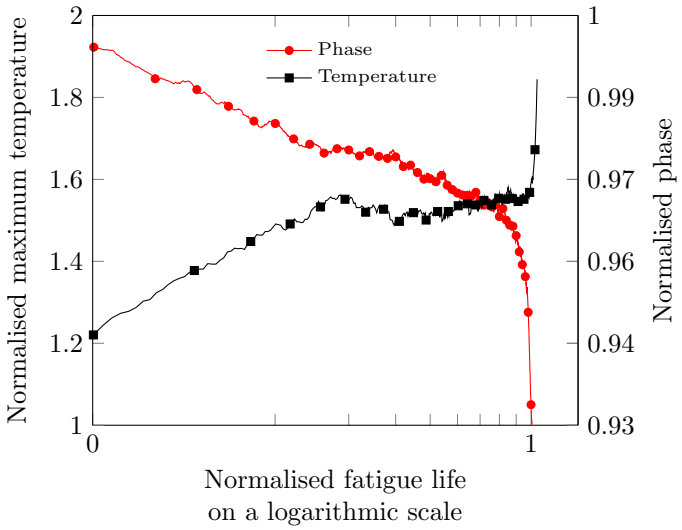

Figure 16: Evolution of the maximum temperature on the surface of the blade and of the response phase.

structural changes than resonance frequency decay. Thus, the resonance phase should be monitored to precisely identify the damage initiation, which leads to small changes in stiffness.

The presented approach provides a tool to identify the critical moment in the fatigue life at which the component undergoes a step change in its mechanical properties. One key application is the detection of the damage initiation in composite materials such as laminated CFRP. For laminated composites, the damage initiation and propagation lead to a continuous structural degradation, without triggering a severe failure, as is the case for metals [27]. Instead, for tests running at resonance, when minor matrix cracks couple together into a major delamination, an abrupt change in dynamic parameters, such as in the response phase, can be found; failure is then defined as the critical event that changes the rate of structural degradation. As a result, S-N curves to delamination initiation can be built rapidly, providing useful data to feed the FE models for predicting the fatigue life. For the experimental outcomes here presented, all the critical events occurred within a response phase change of 5°, related to a stiffness degradation of less than 0.6%. Yet, it is not possible to generalise this threshold to every case without building a critical event data-set.

It was shown that the method is applicable to a general laminate composite specimen and to a complex laminate composite component, indicating that the physics behind the failure of coupons is the same as that behind the failure of real components, irrespectively of the stacking sequence and geometry. The critical event was found to be a well-defined point in the fatigue life of a composite laminate featuring ply-drops, defining the transition between zero damage tolerance and damage propagation. However, the presence of ply-drops does not allow for these conclusions to hold a priori for any case, even though there are numerous examples where ply-terminations are unavoidable for cross-section variations in real components. Nevertheless, the authors showed that the phase response is highly sensitive for monitoring damage development and structural degradation, irrespective of the existence of a critical event.

Acknowledgements

The authors acknowledge Rolls-Royce plc. for supporting and funding the research programme focussed on HCF resonant testing of composites.

References

[1] B. Bhattacharya. Continuum damage mechanics analysis of fatigue crack initiation. *International Journal of Fatigue*, 20(9):631–639, 1998.

[2] M. D. Sangid. The physics of fatigue crack initiation. *International Journal of Fatigue*, 57:58–72, 2013.

[3] K. Reifsnider. Fatigue behavior of composite materials. *International Journal of Fracture*, Vol. 16(6):563–583, 1980.

[4] A. Caiulo and M. Kachanov. On Absence of Quantitative Correlations Between Strength and Stiffness in Microcracking Materials. *International Journal of Fracture*, 164(1):155–158, 2010.

[5] M. J. Salkind. Fatigue of composites. *Composite Materials Testing and Design (2nd Conf), ASTM STP 497, American Society for Testing and Materials*, pages 143–169, 1972.

[6] S. V. Lomov et al. Experimental methodology of study of damage initiation and development in textile composites in uniaxial tensile test. *Composites Science and Technology*, 68(12):2340–2349, 2008.

[7] M. Quaresimin and M. Ricotta. Fatigue behaviour and damage evolution of single lap bonded joints in composite material. *Composites Science and Technology*, 66(2):176–187, 2006.

[8] O'Brien, T. K. Towards a Damage Tolerance Philosophy for Composite Materials and Structures. In *Composite Materials: Testing and Design (Ninth Volume), ASTM STP 1059*, pages 7–33. 1990.

[9] G. D. Sims. Fatigue test methods, problems and standards. In Brian Harris, editor, *Fatigue in Composites*, chapter 2, pages 36–62. Whoodhead Publishing Limited, 2003.

[10] ISO 13003 - Fibre reinforced plastics - Determination of fatigue properties under cyclic loading conditions, 2003.

[11] M. May and S. R. Hallett. A combined model for initiation and propagation of damage under fatigue loading for cohesive interface elements. *Composites Part A: Applied Science and Manufacturing*, 41(12):1787–1796, 2010.

[12] T. K. O'Brien and K. Reifsnider. Fatigue Damage Evaluation through Stiffness Measurements in Boron-Epoxy Laminates. *Journal of Composite Materials*, 15(1):55–70, Jan 1981.

[13] M. May and S. R. Hallett. An assessment of through-thickness shear tests for initiation of fatigue failure. *Composites Part A: Applied Science and Manufacturing*, 41(11):1570–1578, 2010.

[14] D. Di Maio and F. Magi. Development of testing methods for endurance trials of composites components. *Journal of Composite Materials*, 49(24):2977–2991, 2015.

[15] S. Han et al. Vibration fatigue analysis for multi-point spot-welded joints based on frequency response changes due to fatigue damage accumulation. *International Journal of Fatigue*, 48:170–177, 2013.

[16] P. Lorenzino and A. Navarro. The variation of resonance frequency in fatigue tests as a tool for in-situ identification of crack initiation and propagation, and for the determination of cracked areas. *International Journal of Fatigue*, Aug 2014.

[17] B. Lazan et al. Dynamic testing of materials and structures with a new resonance-vibration exciter and controller. Technical report, Wright Air Development Center, Ohio, 1952.

[18] M. Traupe, J. Hug, and H. Zenner. Variable Amplitude Loading on a Resonance Test Facility. *Journal of ASTM international*, 1(10):1–14, 2004.

[19] O. Kováík et al. Resonance bending fatigue testing with simultaneous damping measurement and its application on layered coatings. *International Journal of Fatigue*, 2015.

[20] Daniel Backe, Frank Balle, and Dietmar Eifler. Fatigue testing of CFRP in the Very High Cycle Fatigue (VHCF) regime at ultrasonic frequencies. *Composites Science and Technology*, 106:93–99, jan 2015.

[21] F. Magi, D. Di Maio, and I. Sever. Development of a testing method for vibration fatigue at resonance. In *20th International Conference on Composite Materials*, Copenhagen, July 2015.

[22] R. Talreja. Transverse Cracking and Stiffness Reduction in Composite Laminates. *Journal of Composite Materials*, 19(4):355–375, 1985.

[23] N. G. Stephen. On energy harvesting from ambient vibration. *Journal of Sound and Vibration*, 293(1-2):409–425, 2006.

[24] Hexcel. Hexply 8552 product data. `http://www.hexcel.com/Resources/DataSheets/Prepreg-Data-Sheets/8552_eu.pdf`, 2013.

[25] R. Talreja and C. V. Singh. Damage in composite materials. In *Damage and failure of composite materials*, pages 46–48. 2012.

[26] M. May and S. R. Hallett. An advanced model for initiation and propagation of damage under fatigue loading part I: Model formulation. *Composite Structures*, 93(9):2340–2349, 2011.

[27] P. W. R. Beaumont. Physical modelling of damage development in structural composite materials under stress. In *Fatigue in Composites*, pages 365–412. Elsevier, 2003.